The Pennsylvania State University

The Graduate School

DEVELOPMENT OF EXPERIMENTAL METHODOLOGY TO DETERMINE THE HEAT TRANSFER OF ADDITIVELY MANUFACTURED AIRFOIL CHANNELS IN A HIGH-SPEED LINEAR CASCADE RIG

A Thesis in

Additive Manufacturing and Design

by

Justin Wolff

Submitted in Partial Fulfillment

of the Requirements

for the Degree of

Master of Science

December 2022

The thesis of Justin R. Wolff was reviewed and approved by the following:

Karen A. Thole
Department of Mechanical Engineering
Distinguished Professor
Thesis Co-Advisor

Stephen P. Lynch
Department of Mechanical Engineering
Associate Professor
Thesis Co-Advisor

Reid Berdanier
Associate Research Professor

Allison M. Beese
Department of Materials Science and Engineering
Department of Mechanical Engineering
Associate Professor
Director of Additive Manufacturing and Design Program

ABSTRACT

A developed methodology for determining the internal heat transfer coefficient within a high speed linear cascade rig at steady state conditions is proposed. The methodology outlined in this study is essential to an end goal of rapid concept selection of internal cooling schemes for gas turbine engine applications. Additive manufacturing played an important role in the development and complex instrumentation of linear cascade, airfoil hardware. Additionally, additive manufacturing methods support the goal of rapid concept selection due to the advantage of having a quick turnaround time in comparison to traditional airfoil manufacturing methods. The multiple cascade hardware sets that were developed each implement a different internal cooling channel design scheme. The complex instrumentation that was designed into the hardware, via additive manufacturing, was utilized to evaluate and compare heat transfer and friction factor effects. A computational analysis tool was used to produce mock test data of the cascade hardware, which allowed for the development of the heat transfer methodology via data reduction. The heat transfer and friction factor results from CFD were compared to the methodology data reduction and an agreement between the two was identified; a 0.2% difference in internal heat transfer coefficient was found. The validation of the methodology via computational means is an essential step toward linear cascade testing validation. Testing of a baseline, empty microchannel cascade hardware is underway to achieve full-fledged validation of the proposed methodology. Preliminary friction factor results indicate agreement with literature for channels that have similar hydraulic diameters, whereas heat transfer results indicate the need for further development due to obstacles impacting repeatability.

TABLE OF CONTENTS

LIST OF FIGURES v

NOMENCLATURE vi

ACKNOWLEDGEMENTS vii

Chapter 1 Development of Experimental Methodology to Determine the Heat Transfer of Additively Manufactured Airfoil Channels in a High-Speed Linear Cascade Rig 1

1.1 Introduction 1
1.2 Literature Review 3
1.3 Description of Hardware 8
1.4 Data Reduction Methods 13
Simulation Test Setup and Data Collection 13
Heat Transfer 16
Pressure Loss 19
IR Calibration 20
1.5 Results 22
1.6 Conclusion 27

References 29

LIST OF FIGURES

Figure **1-1**: Linear cascade airfoil hardware a) example of printed hardware from Rusted and Lynch [12] study with a single central test airfoil; b) current study hardware with three central test airfoils. 10

Figure **1-2**: Example cartoon airfoil with static pressure tap locations. 10

Figure **1-3**: Temperature and pressure instrumentation of the cooling blade, baseline hardware was designed with additive manufacturing and heat transfer analysis in mind 12

Figure **1-4**: Cooling design schemes each implemented into the microchannels of seven unique linear cascade hardware pieces. 13

Figure **1-5**: The 3D conjugate CFD analysis that included the gas path boundaries (shown) and an airfoil with an empty microchannel cooling design. 15

Figure **1-6**: The control volume for the developed heat transfer methodology. 16

Figure **1-7**: The developed IR camera calibration insert. 20

Figure **1-8**: Pressure side dewarped IR spatial calibration image. 21

Figure **1-9**: IR camera temperature calibration data and trendline information for the pressure side of the airfoil. 22

Figure **1-10**: a) CFD defined internal and external surface temperature lines b) CFD defined cross-sectional planes for mean air temperature calculation. 23

Figure **1-11**: Comparison of methodology to CFD regarding temperature analysis of channel 2. 24

Figure **1-12**: Three test day results of channel 2 normalized friction factor over a range of Reynolds numbers. 25

Figure **1-13**: Three test day results of channel 3 normalized friction factor over a range of Reynolds numbers 25

Figure **1-14**: Three test day results of channel 2 normalized Nusselt number over a range of Reynolds numbers. 26

Figure **1-15**: Four test day results of channel 3 normalized Nusselt number over a range of Reynolds numbers. 27

NOMENCLATURE

A_c	channel cross-sectional area
c_p	specific heat
D_h	hydraulic diameter
f	friction factor
f_0	friction factor, smooth pipe
H	blade height or channel length
h_1	external heat transfer coeff.
h_2	internal heat transfer coeff.
k	conductivity
$\dot{m}$	mass flow rate
Nu	channel Nusselt number
Nu_0	Nusselt, smooth pipe
P	channel perimeter
p	channel perimeter
P_{base}	pressure at channel inlet
Pr	Prandtl number, $Pr = \frac{\mu c_p}{k}$
P_{tip}	pressure at height H
ΔP	pressure drop
Q	total heat transfer
q”	heat flux
R_{cond}	conduction resistance term
Re	cascade exit Reynolds number
Re_D	channel Reynolds number
R_{ext}	external convection resistance term
R_{int}	internal convection resistance term
R_{total}	total resistance term
t	wall thickness
T_∞	cascade inlet total temp.
T_m	mean channel air temp.
$T_{m,i}$	mean inlet air temp.
T_s	blade surface temp.
$T_{s,ext}$	external wall temp.
$T_{s,int}$	internal wall temp.
U	overall heat transfer coeff.
v	velocity

Greek Symbols

μ	dynamic viscosity
ρ	density

ACKNOWLEDGEMENTS

I would like to acknowledge my advisors Dr. Karen Thole and Dr. Stephen Lynch. The guidance and knowledge that they have both given me has substantially prepared me for my future engineering career. I would also like to thank my fellow START/ExCCL graduate students for their support during my time as a research assistant.

This work was performed under Cooperative Agreement 13-C-AJFE-PSU, Amendments 054 and 065, funded by the Federal Aviation Administration. Any findings or conclusions are those of the researchers and do not necessarily reflect the view of the Federal Aviation Administration.

Chapter 1

Development of Experimental Methodology to Determine the Heat Transfer of Additively Manufactured Airfoil Channels in a High-Speed Linear Cascade Rig

1.1 Introduction

Internal cooling within gas turbine blades continues to be a necessity for longevity due to the high temperatures introduced by the combustion process. Double-wall internal cooling is extensively used within modern-day gas turbine blade designs, as double-wall schemes generally surpass that of the cooling effects of traditional techniques. Double-wall cooling techniques typically make use of impingement and film cooling geometries. Impingement holes in a double-wall cooling scheme traditionally feed cooling flow from a center cavity to the backside of a microchannel outer wall, whereas film holes create a cooled boundary around the external surface of the outermost wall. The combination of these two cooling techniques in a double-wall design, as well as the implementation of microchannel internal cooling schemes like pin fins and ribs, thoroughly boosts cooling performance within gas turbine blades. The manufacturing of gas turbine blades has traditionally followed an investment casting process, where molds are used to produce the final airfoil product. Investment casting begins with creating a wax mold, which is then used to create a mold out of ceramic material.

Once the ceramic material is hardened and sets, the wax is removed via a high temperature burn that evaporates the wax. The ceramic mold is then filled with molten metal to achieve a gas turbine blade. Although, recent trends have shifted toward the use of additive manufacturing in the production of gas turbine blades due to its unique capabilities.

Metal additive manufacturing has been an increasingly utilized technology within the field of turbine design. Advantages of additive manufacturing stem from less waste material, cheaper costs, quicker turnaround time, and a single step manufacturing process (apart from post-processing). Additive manufacturing also has the ability to produce much more complex structures than traditional techniques, such as investment casting. However, minimum feature sizes, post-processing, and surface roughness effects are several areas where researchers need to pay close attention. Although, for many applications, including gas turbine blade design, the ability of rapid prototyping with additive manufacturing and cheaper costs cannot be overlooked.

The current study discusses the development of true engine scale (or 1x scale), additive turbine blade hardware to be used in a high-speed linear cascade rig to investigate novel double wall cooling configurations. Internal cooling designs from public literature have been implemented into the double wall cooling channels. In addition, the current study has developed an experimental methodology that could allow for convective heat transfer and overall pressure drop results to be obtained in-situ in the turbine blade model while it operates in the representative high Mach number environment of the cascade. Computational fluid dynamics (CFD) was used to design and test the proposed methodology and is useful to compare to experimentally obtained results. The developed methodology is advantageous in that it enables the isolation of internal and external heat transfer coefficients from the overall heat transfer coefficient. This capability is important, as the internal heat transfer coefficient is a key metric that will be used to compare the performance of the current study's internal cooling schemes.

1.2 Literature Review

A wide variety of internal cooling scheme studies have been published in literature. Pin fins are of particular interest due to their ability to increase the heat transfer within internal channels, however, there are tradeoffs between heat transfer and associated friction factor. The following are several factors that have an impact on the performance of pin fins in regard to heat transfer and friction factor: pin fin height, streamwise and spanwise spacing, proximity of pin fin array to channel walls, and surface roughness effects. Trends in literature have found that friction factor within a pin fin array is directly associated with the spanwise spacing; as the spanwise spacing of the pin fin array decreases, the pressure drop increases due to the increased blockage to the flow. The paper by Kirsch et al. [1] indicated that this trend was not upheld for additively manufactured, cylindrical pin fin arrays due to the influence of varying surface roughness between test articles. The study illustrated that in comparison to smooth pin fin arrays, the additive arrays saw a much larger increase in friction factor. The paper also produced results associated with the heat transfer effects of additive pin fin arrays. A decrease in the spanwise and/or streamwise spacing of the pin fin array produced an increase in heat transfer. The additive nature of the pin fin array in the Kirsch et al. [1] study also identified additive pin fin arrays as having a larger influence to heat transfer than smooth channels due to surface roughness.

Other factors that have an influence on the heat transfer and friction factor performance of pin fins revolve around the pin fin shape used. A study by Ferster et al. [2] analyzed the effects of varying additive pin fin geometries. The pin fin geometries that were studied included triangle pin fins (flat face toward and away from the flow), star pin fins, and dimpled-sphere pin fins. Each pin fin geometry was investigated thoroughly by adjusting the spacing and numbering of pin fins among several test cases. The results of the study indicated that pin fin geometry had the largest impact on heat transfer and friction factor effects when compared to the spacing of the pin

fin arrays. Triangular pin fins with the flat edge facing the flow had the highest heat transfer augmentation. The Ferster et al. [2] study also led to the conclusion that streamwise spacing had little effect on friction factor but increased heat transfer with decreased streamwise spacing. Impacts of additive manufacturing, spacing, and pin fin geometries are key areas to uncover when determining how to design pin fin geometries into an internal cooling channel. Specifically, a balance between heat transfer and friction factor must be met, as some applications may allow for higher friction factor as opposed to others.

Not only are pin fins of interest in literature and turbine cooling applications, turbulators or ribs are sought after as well due to their ability to increase cooling performance. Similar to that of pin fin arrays, the heat transfer and friction factor impacts of rib cooling schemes depend on dimensions and spacing. Critical areas of rib design that influence heat transfer and friction factor include rib geometry, pitch, height, angular dimensions, staggering, and channel aspect ratio. A study by Wright et al. [3] investigated the performance of angled, v-shaped, and w-shaped ribs with a 4:1 channel aspect ratio. Each of the studied rib geometries were also adjusted to obtain results of discrete or staggered ribs, where each row of ribs is halved and shifted slightly upstream and/or downstream. Results of the study identified v-shaped and w-shaped ribs as having the best thermal performance, where the w-shaped and discrete-w shaped ribs produced the largest heat transfer and friction factor. Wright et al. [3] also discussed trends typically seen when altering channel aspect ratio; a decrease in aspect ratio (i.e. from 4:1 to 2:1) increases heat transfer. In addition, the literature suggests that a pitch to rib height ratio of 10 is optimal for cooling performance.

More complex rib geometries bring new discussions of optimal dimensions for cooling performance. One such rib design, a boot-shaped rib, was evaluated by Dinh et al. [4]. The paper discusses the heat transfer and friction factor impacts of a boot-shaped design versus a typical square rib geometry. Additional variables that were varied include: boot heel and toe angle, boot

slope height, and rib width. Results of the study identified high heat transfer at the rear region of the boot and determined that rib-width had no significant effect on heat transfer when compared to the other boot dimensions; the highest thermal performance was seen with a boot heel angle of 30 degrees. This study by Dinh et al. [4] indicates the importance of due diligence research for more complex, novel rib schemes, as this is a necessity for the advancement of internal cooling in general.

Bounds toward other complex internal cooling methods have been made, specifically in the area of wavy channel schemes. Internal cooling geometries have a significant impact on the heat transfer and friction factor characteristics of a given application. Instead of investigating geometries to be placed within a cooling channel, the study by Kirsch et al. [5] sought to analyze the effects of altering the entire cooling channel geometry itself by evaluating an additively made wavy channel. The study focused on adjustments to the wavelength of a wavy channel to identify heat transfer and friction factor performance trends. Three different wavelengths (10%, 20%, and 40% of a wavelength period) were evaluated and compared to each other and to a rectangular, straight cooling channel design. Results indicated that the channels with 20% and 40% of a wavelength period had better heat transfer and slightly worse friction factor performance compared to a straight channel design. These longer wavelengths allowed for the coolant to stay close to the channel wall boundary, whereas the channel with 10% of a wavelength period saw the coolant flow pulling away from the walls that led to a much higher friction factor result. Another trend that was identified was that the Nusselt number augmentation, for the channels with 20% and 40% of a wavelength period, was significant for Reynolds numbers less than 4000.

Another study researched the wavy channel space to further evaluate the effects of not only wavelength but amplitude as well. The paper by Corbett et al. [6] investigated five different additively manufactured wavy channel designs, each of which with a variety of wavelength and amplitude definitions. Per the results, a decrease in channel wavelength or increase in amplitude

boosted heat transfer performance while increasing friction factor. Additionally, trends of large increases in friction factor due to increased waviness was observed; heat transfer increased in association with increased waviness as well but not as significantly as friction factor.

Increased complexity in overall airfoil design has led to improved cooling performance as well, specifically in the implementation of double wall cooling. Double wall cooling has been frequently studied and utilized in literature due to its ability to draw improved cooling performance aspects from both impingement and film cooling. Separately, impingement cooling and film cooling have been extensively studied for use in turbine cooling applications. However, trends toward combining these techniques have led to much improved cooling performance. A study by Huelsmann et al. [7] investigated convective heat transfer effects of impingement jets on effusion (or film cooling) holes. Experimentation was set up to test the effects of varying the impingement hole angular and circumferential position in regard to two separate effusion holes of different lengths. The testing specimens were produced via additive manufacturing and a constant heat flux was applied to the test articles for heat transfer evaluation. The overall trend identified by this study was that impingement holes produce 10-30% more heat transfer in combination with the effusion holes depending on the impingement location. Therefore, an important takeaway of double wall techniques is that impingement hole placement is key to receiving the most efficient cooling performance.

Additional studies, such as the paper by Hossain et al. [8] investigate double wall cooling and internal cooling geometries (i.e. pin fins) in concert. The study incorporates these internal and external designs via additive manufacturing in a 1x, engine scale nozzle guide vane. Both a double wall and single wall vane were produced and tested to evaluate the Nusselt number augmentation achieved. Two pin fin arrays were implemented into the double wall and single wall vane separately, where only the double wall vane experienced impingement cooling. One such pin fin array included circular pin fins, whereas the other saw a triangular pin fin design.

Transient heat transfer experiments were run to produce resulting indicating that heat transfer augmentation is higher for the triangular pin-fin array design as opposed to the circular pin fins. The triangular double wall scheme also produced a larger Nusselt number augmentation and lower friction factor augmentation than that of its single wall counterpart.

Transient methods of internal heat transfer analysis have been found in literature, however, methodology for steady state heat transfer analysis tends to be an area of uncertainty. The main purpose of the current study is to provide in-situ measurements of heat transfer through an internally cooled channel by linear cascade, steady state means. An example of a transient method that has been developed for the purpose of internal heat transfer evaluation is the non-destructive technique introduced by Nirmalan et al. [9]. The method by Nirmalan et al. [9] makes use of an IR camera for data collection of a transient airfoil test and utilizes 3D inverse transient conduction and finite element analyses for an iterative solution process. Once the finite element analysis temperatures match that of the measured temperatures, the correct internal heat transfer coefficient distribution is achieved. A comparative process can be illustrated through the study by Egger et al. [10], where again a transient method for determination of internal heat transfer coefficients is proposed. In this case, Egger et al. [10] introduce a lumped capacitance method, where an energy balance is applied to correlate the sum of internal convection, conduction, natural convection, and radiation to the transient energy storage. The lumped capacitance data reduction leads to a need to determine two coefficients through the use of obtained IR camera data, where an iterative process is imposed via boundary condition and initial condition adjustments.

A common trend of internal heat transfer analysis methodologies in literature indicates the use of transient testing as well as an iterative solution process. The current study aims to produce a straightforward methodology for determining the heat transfer of internal cooling channels via a steady state technique. Overall cooling effectiveness of additively manufactured

double wall cooling designs is being investigating via this methodology. Double wall cooling and novel internal cooling geometries, and schemes, are being combined in a single study to determine if a larger enhancement of cooling performance is observed. The proposed methodology not only allows for the internal convection coefficient to be obtained for additively made turbine blade microchannels, the testing setup also allows for the determination of friction factor results. Therefore, a complete analysis of the Nusselt number and friction factor augmentation of incorporated internal cooling schemes can be performed.

1.3 Description of Hardware

The transition between investigations of turbine blade internal cooling schemes at a low testing readiness levels and high readiness levels can be achieved via Penn State' high speed linear cascade rig. Penn State's linear cascade enables 1x scale 2D airfoil geometries to be tested, specifically for the purpose of quick, efficient evaluation of internal cooling geometries within the present study. Internal cooling learnings achieved via linear cascade testing provides a needed filter for cooling design concepts that may be implemented into turbine rig testing. The capabilities of the Penn State high-speed linear cascade include the ability to run a wide range of Mach number and Reynolds number conditions at steady conditions [11], which is advantageous in the collection of a variety of test data for turbine airfoils. Additional capabilities of the linear cascade include optical windows for IR camera usage and a turntable for incidence angle adjustments of the cascade, airfoil hardware. The design of the linear cascade hardware and the flow field benchmarking process of the current study follows a process as shown by Rusted and Lynch. [12]. The process of hardware development for the linear cascade has been streamlined by the use of metal additive manufacturing for complex instrumentation, such as routing of pressure taps, can be achieved. Additive manufacturing enables complex instrumentation to be designed

into the linear cascade hardware as well as complex internal cooling schemes. Not only can complex designs be produced, they can be efficiently manufactured for rapid prototyping.

A 1x scale, additive linear cascade blade row with seven 2D airfoils was developed to verify the flow field of the airfoil geometry within the high speed linear cascade. Figure 1-1a shows an example of a public airfoil set that has been used in the study by Rusted and Lynch [12]. The current study's hardware was designed as indicated by Figure 1-1b. The three center airfoils are removable, which allows for a variety of hardware pieces to be efficiently interchanged for flow field and internal cooling tests. The hardware for the flow field validation was designed to obtain static pressure measurements around the mid-span of all seven airfoils in the blade pack. Pressure taps were utilized to collect the pressure data, where the pressure tap locations were selected based on the pressure loading curve from a 2D computational analysis of the airfoil geometry. Figure 1-2 illustrates a cartoon example airfoil geometry (not representative of the actual airfoil shape due to proprietary limitations) with similar pressure tap locations to that of the current application's center three airfoils. A larger number of pressure tap locations were designed around the perimeter of the center three airfoils. Due to optical limitations of the infrared camera setup, cooling features were only located in the center airfoil, but it was important to establish the periodicity of the flow on all airfoils around that central one.

The validation of the linear cascade flow field was performed at six testing conditions. The testing matrix included three different cascade Mach number conditions: 0.7, 0.81, and 0.9. Testing for each Mach number condition was performed at a no back pressure Reynolds number condition as well as an ADP, and high Reynolds number condition. Static pressure data was collected and averaged over a 1 minute interval, with five repeat tests performed for each condition to ensure repeatability. The pressure results for the centermost airfoil were compared to that of the 2D periodic computational analysis used to design the airfoil and showed less than 2% difference for each pressure tap location.

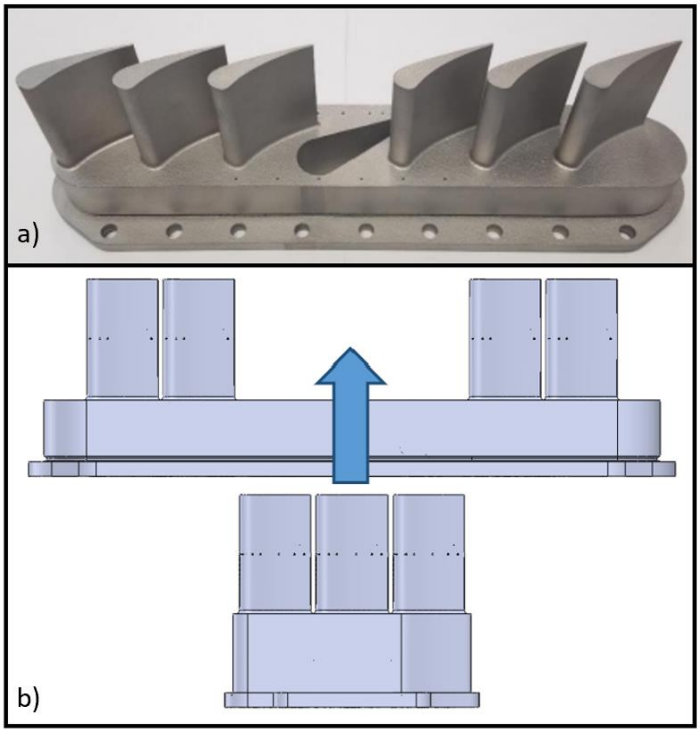

Figure **1-1**: Linear cascade airfoil hardware a) example of printed hardware from Rusted and Lynch [12] study with a single central test airfoil; b) current study hardware with three central test airfoils.

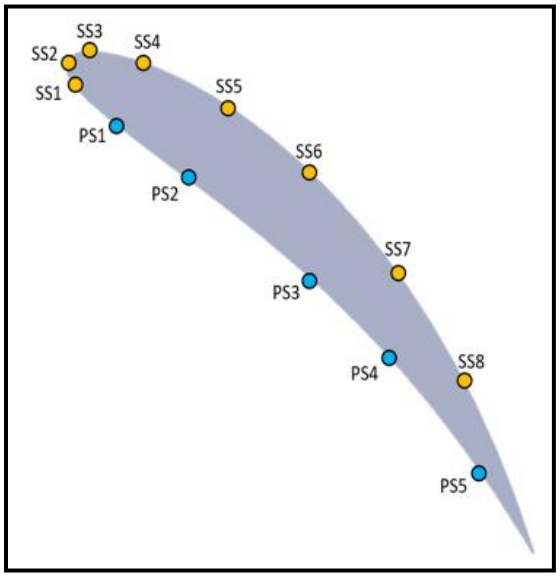

Figure **1-2**: Example cartoon airfoil with static pressure tap locations.

A linear cascade hardware piece with empty microchannels was developed to be a baseline for the internal cooling tests, as shown in Figure 1-3. The baseline hardware makes use of additive's capability to manufacture complex structures, as avenues for instrumentation and cooling channels were routed within the hardware piece itself. Four cooling channels were included in the baseline design, where each channel is defined from the base of the center-most blade (blade 4 in Figure 1-3), to the tip. Cooling channel 1 is located around the leading edge of the blade, cooling channels 2 and 3 are located around the pressure side, and cooling channel 4 is located along the suction side. During testing, each microchannel is fed with cooling flow from the base of the hardware out through the tip of blade 4.

Passageways for pressure tap instrumentation were developed into the base and tip of each channel with the purpose of measuring pressure drop across the microchannels during testing. Holes for sheathed thermocouples were designed into the base of each channel, whereas wire thermocouples were necessary for the tip of each channel to consolidate space. During the design phase of the cascade hardware, it was identified that passageways to the tip of each channel for both pressure taps and thermocouples was unrealistic. Due to the thin nature of the airfoil geometry, only one passage per channel was able to be designed with the appropriate clearance necessary for additive manufacturing. The avenues that were designed to the tip of each channel were selected as pressure tap instrumentation, whereas another method was explored for temperature measurements at the tip of each channel. The deduced method, which may require more investigation, was to route wire thermocouples from the tip of each channel, over the tip gap, and out the back of the linear cascade. The thermocouple instrumentation enables the cooling air temperature at the base and tip of each channel to be determined during testing for use in heat transfer analysis.

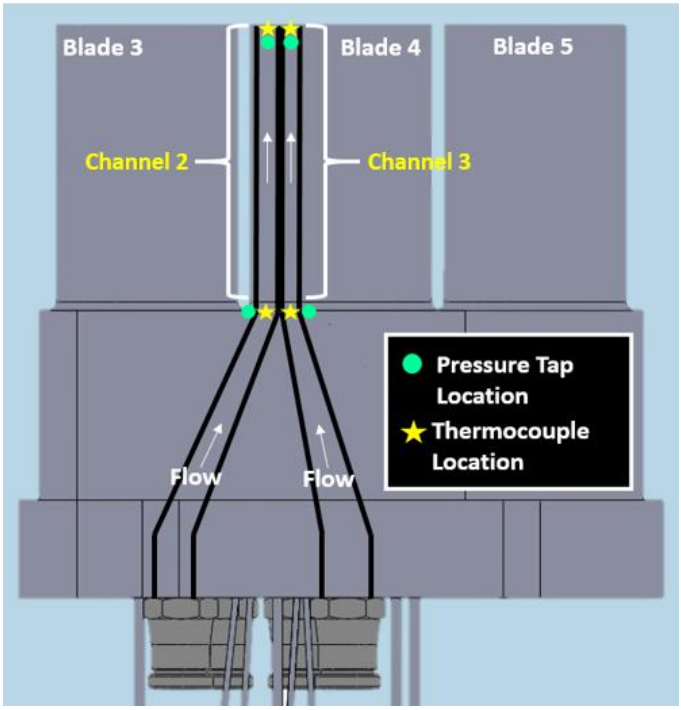

Figure **1-3**: Temperature and pressure instrumentation of the cooling blade, baseline hardware was designed with additive manufacturing and heat transfer analysis in mind.

In addition to a baseline empty microchannel configuration, various internal cooling enhancement schemes were placed inside each of the four microchannels in the center blade. The seven implemented cooling schemes were divided into three categories: pin fins, ribs, and empty channel schemes. Figure 1-4 illustrates seven cooling schemes that were each designed into a separate piece of linear cascade hardware, which includes the baseline, empty channel design (design #6). A variety of cooling schemes were selected to that range from conventional cooling features to novel cooling designs. The conventional cooling schemes include cylindrical pin fins, discrete W ribs, and the baseline empty channel design. More novel cooling schemes include triangle pin fins, wavy channels, and wavy ribs.

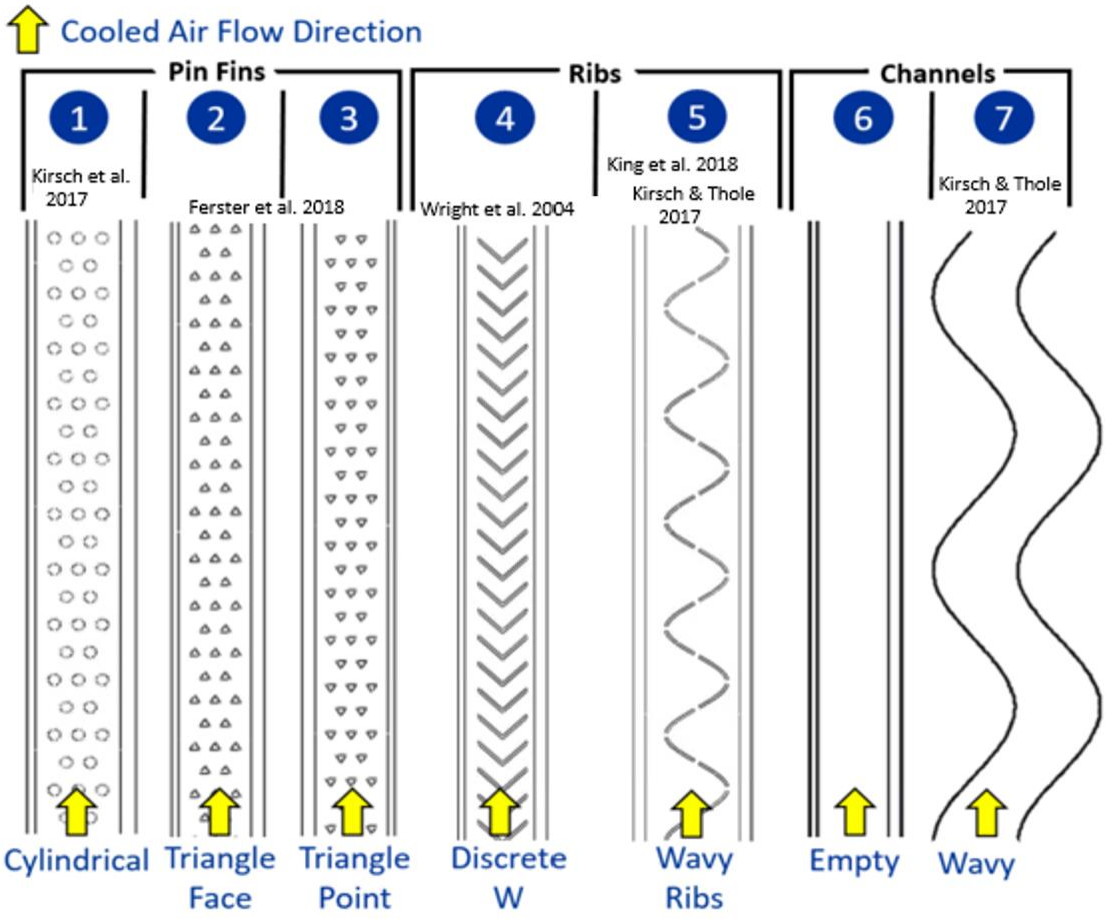

Figure **1-4**: Cooling design schemes each implemented into the microchannels of seven unique linear cascade hardware pieces.

1.4 Data Reduction Methods

Simulation Test Setup and Data Collection

Given the uniqueness of the current experimental setup (additively printed airfoils with novel internal microchannel cooling features), it was desired to be able to characterize the internal convection coefficients in situ. To this end, a methodology was developed to obtain overall

convection coefficients as well as internal and external convection coefficients, using the instrumentation designed into the hardware and the infrared camera surface measurements. To understand the feasibility of the methodology and get an understanding of uncertainties, a computational tool, StarCCM+, was utilized to collect simulated test data for the purpose of developing the data reduction process prior to testing the cascade hardware.

Figure 1-5 shows the empty channel cooling design CFD geometry. The 3D computational analysis was organized to include both a fluid-air and solid-blade domain, an inlet and outlet condition for the cascade airflow, two periodic boundary conditions, and cooling air conditions for each of the four cooling channels. To achieve an accurate computational study, an in depth meshing analysis was performed on the CFD geometry from Figure 1-5. Four meshes were created, from a very coarse to very fine mesh, to be analyzed for use. Selection of the appropriate mesh depended on data collected from each mesh's computational analysis, some of which included: airfoil pressure loading, cascade total temperature, blade surface temperature, and the mean air temperature of each cooling channel. One of the key observations that needed to be made in selecting a mesh was to identify the point at which influential data changes a negligible amount from one mesh to another. The finest mesh that was run fit such a description and was selected to be used in all future detailed analyses.

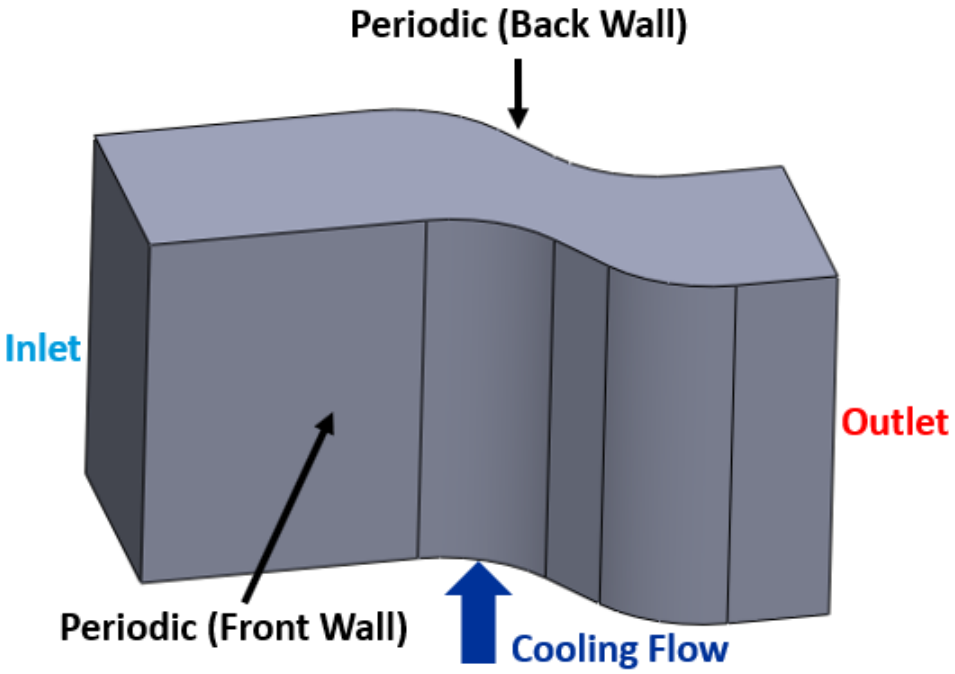

Figure **1-5**: The 3D conjugate CFD analysis that included the gas path boundaries (shown) and an airfoil with an empty microchannel cooling design.

Computational analyses were performed at many different testing conditions including various cascade exit Mach number and exit Reynolds number (Re) conditions; several internal cooling mass flow rate conditions and channel Reynolds numbers (Re_D) conditions were utilized as well. Additionally, each simulation was performed with only one of the four internal channels flowing at a time. The computational results were analyzed, and key assumptions were made to identify the equations necessary to determine both the internal cooling channel heat transfer coefficients (h_2) and the external heat transfer coefficients (h_1).

Heat Transfer

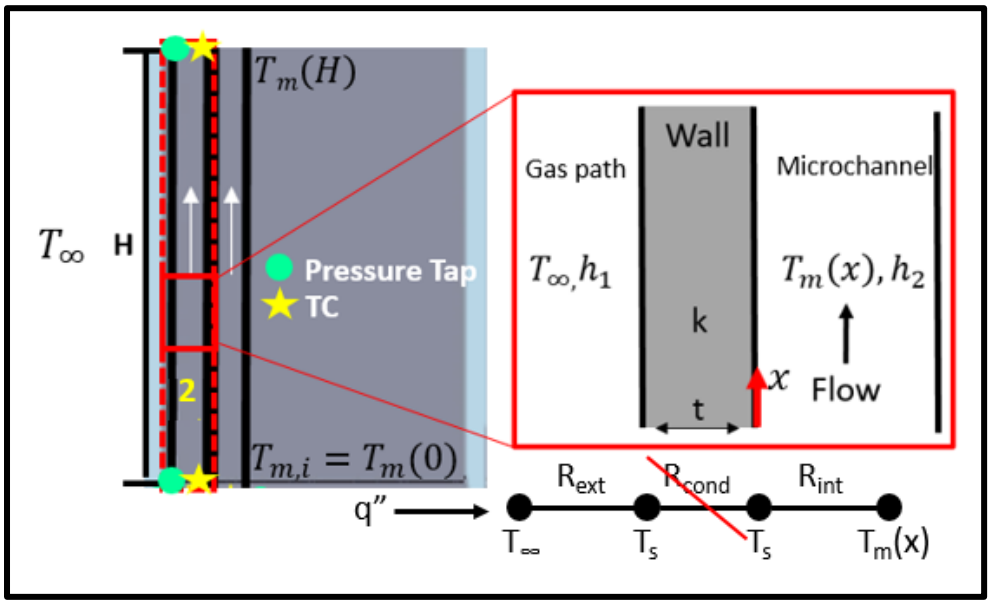

Figure **1-6**: The control volume for the developed heat transfer methodology.

The main objective of the current study is to propose a new methodology for calculating the internal heat transfer coefficient within linear cascade hardware microchannels. The approach to the data reduction process begins with identifying the heat transfer concepts and equation that will be of use. Figure 1-6 illustrates the linear cascade and airfoil hardware system of the present study, where microchannel 2 is being used to show how the system can be evaluated as a circuit. The system is made up of three sections, two of which experience convection where the other sees the influence of conduction. The first section of the circuit analysis explores the convection effects between that of the hot gas path of the linear cascade and the outer wall of microchannel 2. The next section depicts the influence of conduction through the wall of microchannel 2, where material properties and wall thickness play a significant role. The third section identifies the convection effects between the inner wall of microchannel 2 and the cooling flow that is being fed through the channel. Circuit analysis allows for the evaluation of each of these sections as a

system, where the heat flux of the system is defined by the temperatures and resistance terms of each section. The next several paragraphs describe the methodology development process in finer detail.

An overall control volume of the microchannel is used with "measured" inlet and outlet air temperatures and inlet air mass flow rate. From the first law of thermodynamics, the total heat transfer q to the microchannel fluid is defined by Equation 1, where H is the length of the microchannel and T_m is the bulk mean temperature of the microchannel fluid.

Analyzing a differentially long segment of the microchannel wall, the local heat flux (q", or heat transfer rate per unit area of the microchannel wall surface) can also be determined by a steady state thermal resistance network between the outer gas path and the microchannel bulk mean temperature. The thermal resistances (in Fig. 1-6) are: external convection in the gas path (Eq. 2) conduction through the microchannel wall (Eq. 3), and convection inside the microchannel (Eq. 4). From the thermal resistance network, two equations that describe the heat flux at that location can be written (Eq. 6), which relate the temperature difference between the gas path and the wall (using the external convection) to the temperature difference between the gas path and the microchannel bulk mean temperature (using the overall resistance). This can be rewritten as shown in Equation 7, which provides more directly the external convection coefficient (h_1).

Since the determination of the external convection coefficient (h_1) in Equation 7 depends on knowing the value of the overall heat transfer coefficient (U), Equation 8 was used to evaluate the system via internal pipe flow concepts. From knowing the overall heat transfer coefficient (U) and the external convection coefficient (h_1), the internal convection coefficient (h_2) is obtainable via the relationship in Equation 9. For expressing the internal heat transfer non-dimensionally, the Nusselt number can be calculated as indicated by Equation 10, where a comparison to a smooth

pipe of circular cross section can be made via the evaluation of Nu_0 from the Dittus-Boelter equation (Eq. 11).

$$q = \dot{m}c_p(T_m(H) - T_m(0)) \quad (1)$$

$$R_{ext} = \frac{1}{h_1} \quad (2)$$

$$R_{cond} = \frac{t}{k} \quad (3)$$

$$R_{int} = \frac{1}{h_2} \quad (4)$$

$$R_{total} = R_{ext} + R_{int} \quad (5)$$

$$q" = \frac{T_\infty - T_s}{R_{ext}} = \frac{T_\infty - T_m(x)}{R_{total}} \quad (6)$$

$$q" = h_1(T_\infty - T_s(x)) = U(T_\infty - T_m(x)) \quad (7)$$

$$\frac{T_m(H) - T_\infty}{T_{m,i} - T_\infty} = \exp\left[\left(\frac{-PH}{\dot{m}c_p}\right)U\right] \quad (8)$$

$$h_2 = \frac{1}{\left(\frac{1}{U} - \frac{1}{h_1}\right)} \quad (9)$$

$$Nu = \frac{h_2 t}{k} \quad (10)$$

$$Nu_0 = 0.023 Re_D^{0.8} Pr^{0.4} \quad (11)$$

There are several key assumptions that were made for the developed methodology above, one of which includes negligible temperature variation around the perimeter of a given cooled microchannel. Through the use of the CFD simulation data it was found that the temperature varies by roughly three degrees around the perimeter of a microchannel. The influence of using a constant surface temperature methodology when truly a non-constant wall temperature is observed has yet to be determined. A study is currently being done to identify the impacts that a few degrees have on the internal heat transfer calculation.

A second assumption that was made was negligible lateral variation in the blade surface temperature. The validation of this second assumption concentrated on evaluating the temperature variation along the area of the blade that was adjacent to a cooled channel. The blade surface temperatures around a given cooled channel were collected and the results indicated a negligible percent change in lateral temperature.

The third assumption is that there is negligible conduction loss in the microchannel wall. The conduction resistance term across the blade wall is defined in Equation 3. The blade wall thickness, t, is such a small value that the conduction resistance term is negligible, confirming the assumption of negligible conduction loss across the microchannel wall. To further validate this assumption, Figure 1-11 in the results section plots the inner and outer wall temperatures of channel 2. The plot illustrates how close the inner and outer wall temperatures are.

Pressure Loss

The cooling channel hardware was designed to include pressure taps at the base and tip of each of the internal cooling channels, as shown in Figure 1-6. Equation 14 is used to calculate channel friction factor results, where the pressure drop, ΔP, is an experimentally measured quantity through the embedded pressure tap instrumentation.

$$\Delta P = P_{tip} - P_{base} \tag{12}$$

$$D_h = \frac{4A_c}{p} \tag{13}$$

$$f = \Delta P \frac{D_h}{H} \frac{2}{\rho} \frac{1}{v^2} \tag{14}$$

IR Camera Calibration

The surface temperature data is essential to the methodology that was developed to determine the channel internal heat transfer coefficients. To obtain the surface temperature results during the linear cascade cooling design tests, an IR camera is used. In order for the IR camera to properly calculate the blade surface temperature, it must be calibrated via an additional hardware piece as seen in Figure 1-7.

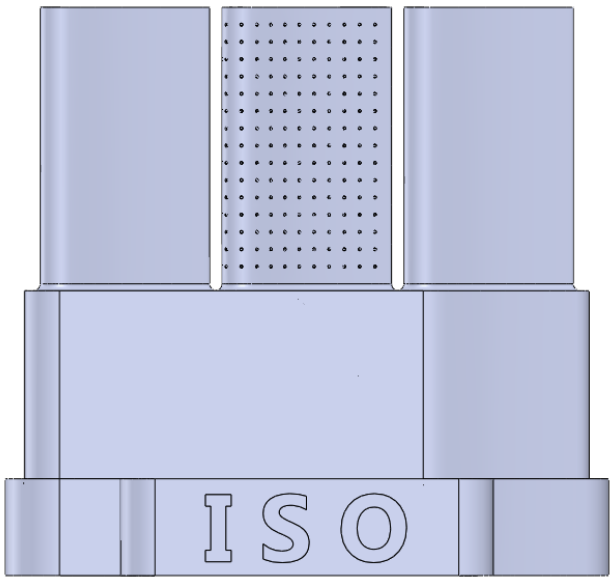

Figure **1-7**: The developed IR camera calibration insert.

Both a spatial and temperature calibration must be performed to fully calibrate the IR camera. To perform the spatial calibration, the calibration airfoil in Figure 1-7 was spray painted black and a silver Sharpie was used to highlight the array of points shown in Figure 1-7. The calibration airfoil was imaged by the IR camera for both a pressure side and suction side view. ResearchIR software was used to select and identify the physical location of the point array. A custom MATLAB code using the Image Processing toolbox was developed to dewarp the 2D image into the coordinate system of the airfoil surface. Figure 1-8 represents a MATLAB

dewarped image of the calibration airfoil's pressure side in the coordinate system of the airfoil, where the dots are the spatial calibration markers showing the dewarping is functioning to recreate a uniform grid.

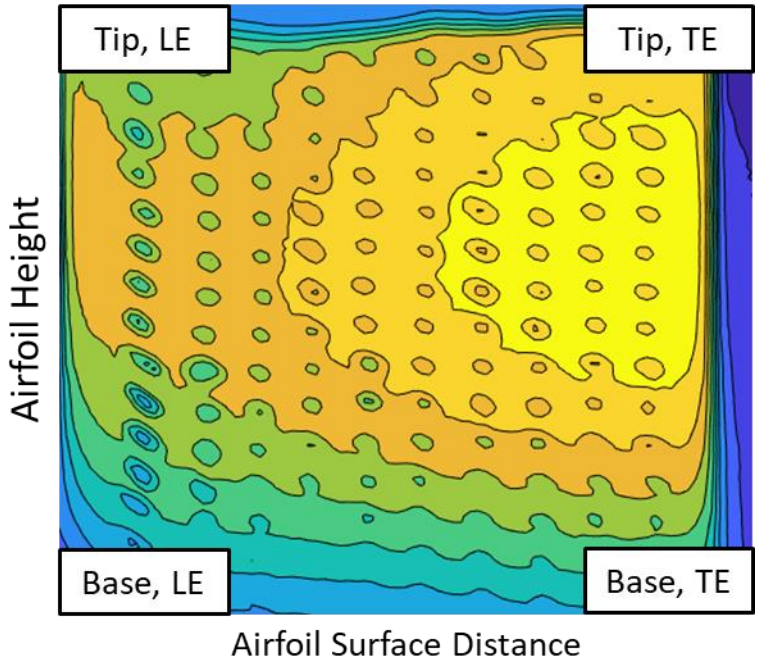

Figure **1-8**: Pressure side dewarped IR spatial calibration image.

An IR camera temperature calibration is necessary as well. The process of temperature calibration involved placing thermocouples at two locations on the surface of the calibration airfoil, two on the pressure and two on the suction side. Surface temperature data at cascade conditions was collected simultaneously using the IR camera and the thermocouples. A comparison between these two sets of data were performed, and the result indicated linear behavior over the range of interest. Figure 1-9 shows data collected for two separate locations on the pressure side of the calibration airfoil. The determined trendlines were used to correct the IR camera temperature data to the true temperature. After calibration, the calibration airfoil is

replaced with cooling design test hardware which is confirmed to be in the same location relative to the camera.

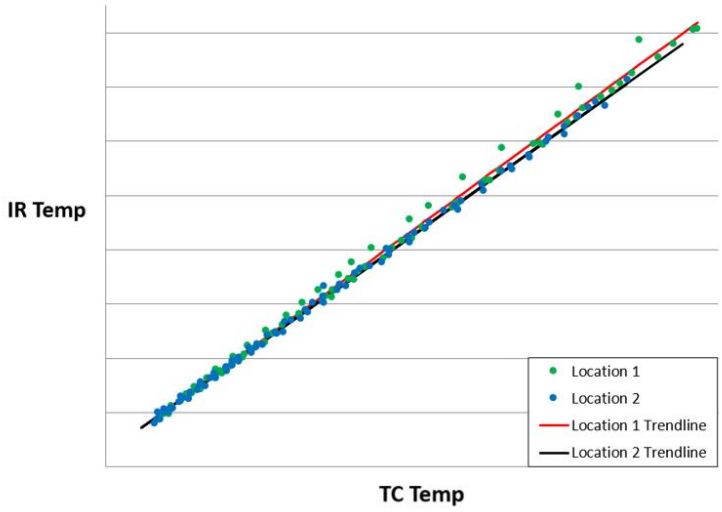

Figure **1-9**: IR camera temperature calibration data and trendline information for the pressure side of the airfoil.

1.5 Results

The heat transfer analysis methodology explained in section 1.4 can be used to determine both the internal and external heat transfer coefficients of the cascade-airfoil. In order to verify the developed methodology, the computational simulation was evaluated as "synthetic" experimental data. Furthermore, initial studies were conducted using the cascade hardware.

The CFD analysis was utilized in creating Figure 1-11, which illustrates a non-dimensional plot of surface temperature and mean cooling air temperature as a function of the height of channel 2. The surface temperature data in Figure 11 was retrieved directly from CFD, where a vertical line along the outer and inner surface of the channel was specified to collect the corresponding data. Figure 1-10a illustrates how a single line was used to extract the outer and

inner surface temperature data of channel 2. The mean cooling air temperature was collected in CFD via twenty sectional planes, which were defined from the base of channel 2 to the tip. A surface average report was created within CFD for each of the channel 2 planes, which allowed for mean air temperature data to be obtained. Figure 1-10b illustrates how the plane sections were defined in the computational program. An additional line that is plotted in Figure 1-11 is the channel 2 mean air temperature, which was calculated via the developed methodology, i.e. Equation 6. The mean temperatures in Figure 1-11 are within a tight margin of one another, which indicates that the developed methodology is accurately calculating the CFD test data results. The inside and outside blade surface temperature results in Figure 1-11 are very similar as well, which reiterates that the negligible conduction loss assumption is valid. The internal heat transfer coefficient was calculated for channel 2 via CFD and via the developed methodology above, as this is an essential metric for comparison. The percent difference between the calculated internal heat transfer coefficients was less than 0.2%, which concludes that the methodology has been computationally verified. However, linear cascade cooling design testing must be completed to completely verify the current method.

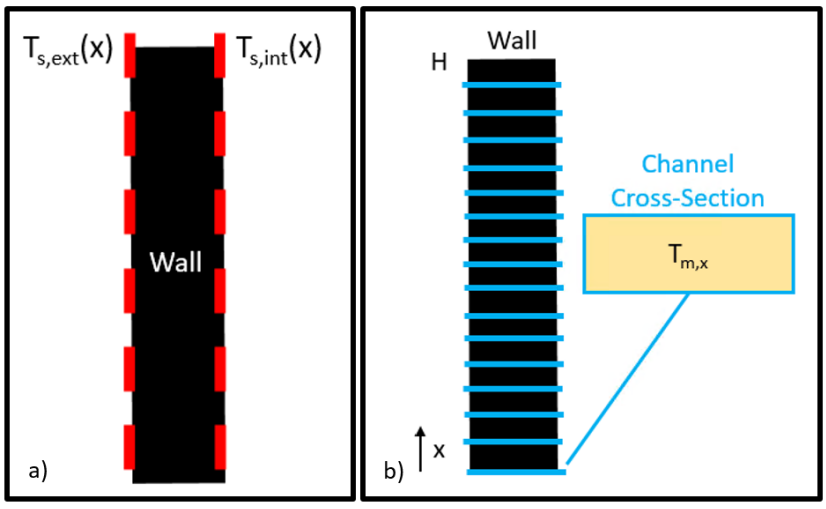

Figure **1-10**: a) CFD defined internal and external surface temperature lines b) CFD defined cross-sectional planes for mean air temperature calculation.

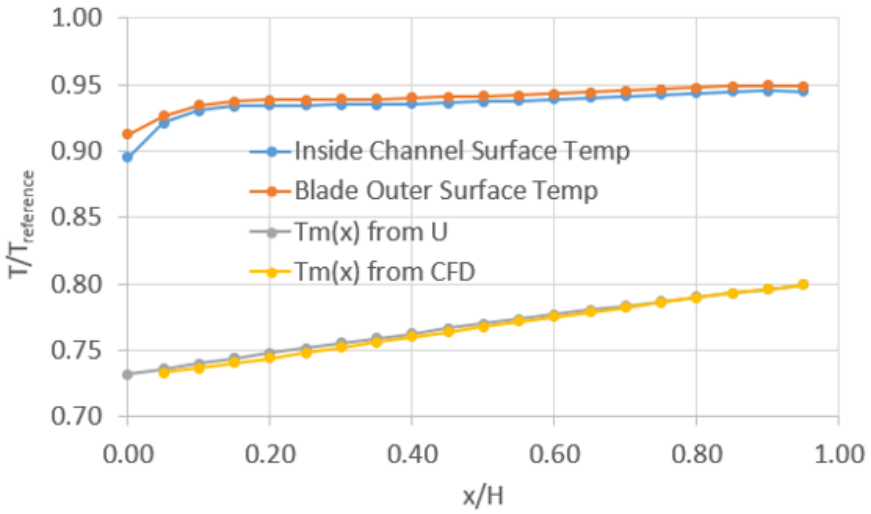

Figure **1-11**: Comparison of methodology to CFD regarding temperature analysis of channel 2.

Testing of the linear cascade empty channel hardware design is currently being performed for the purpose of validating the methodology outlined in the present study. Friction factor results have been obtained for microchannel 2 and 3, as seen in the normalized friction factor plots in Figures 1-12 and 1-13. The plots are normalized via friction factor for smooth pipe flow and the results from Wildgoose et al. [14] and Stimpson et al. [15] studies are plotted for comparison to literature. The friction factor results show good agreement in comparison to the Wildgoose et al. [14] study for channel 3. This is due to the Wildgoose et al. [14] study having channel hydraulic diameters closer to that of channel 3. Agreement to literature indicates that channel 2 and 3 friction factors are properly obtainable through the use of the linear cascade pressure tap instrumentation.

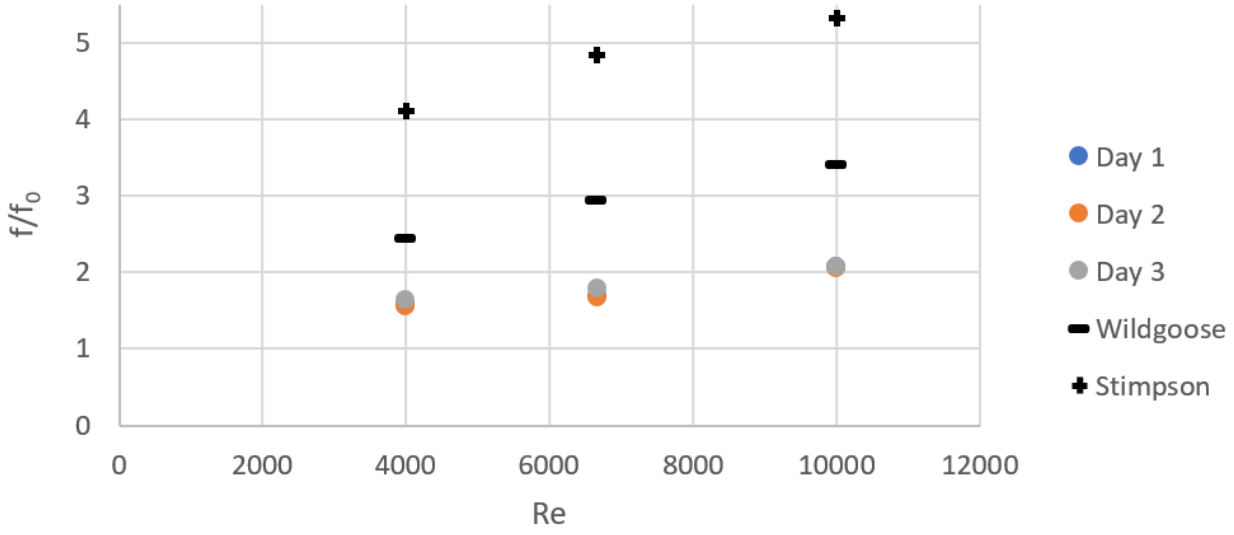

Figure **1-12**: Three test day results of channel 2 normalized friction factor over a range of Reynolds numbers.

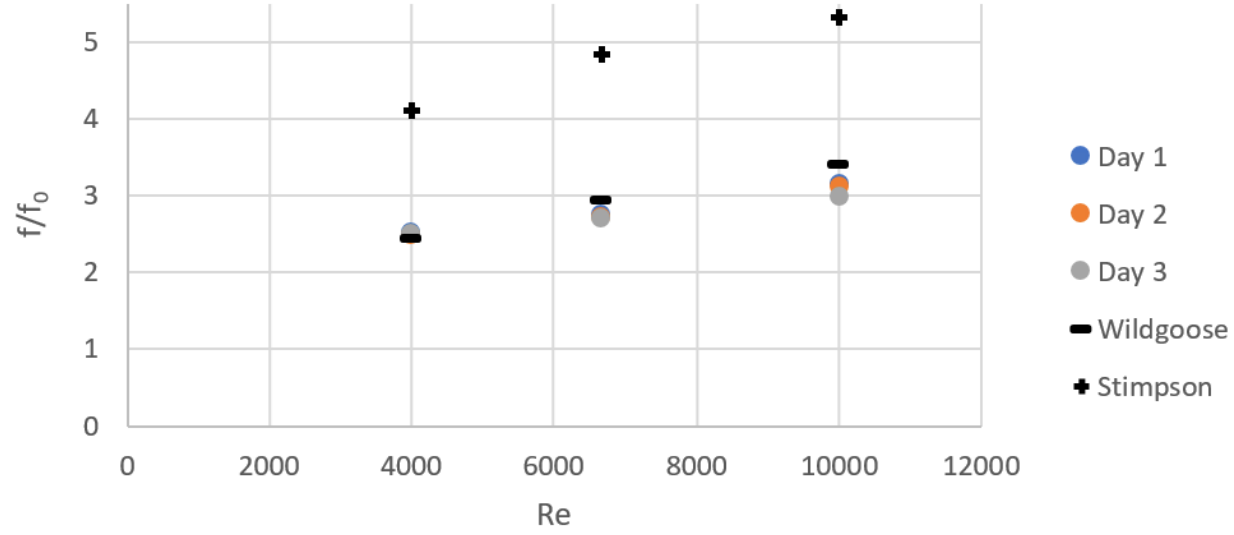

Figure **1-13**: Three test day results of channel 3 normalized friction factor over a range of Reynolds numbers.

Figures 1-14 and 1-15 illustrate normalized Nusselt number results over a range of Reynolds numbers for several test days. The Nusselt number is normalized by Nu_0, which was

determined via the Dittus-Boelter equation for smooth pipe flow. The Nusselt number plots show that Nusselt number fluctuates from one test day to the next. Current challenges with collecting the air temperature at the exit (or tip) of the microchannels exist due to struggles with wire thermocouple placement. The air temperature at the exit of the microchannels directly impacts the Nusselt number because the developed methodology uses this air temperature in the data reduction process. Therefore, future work will focus on developing a more accurate measurement technique for the channel exit thermocouples.

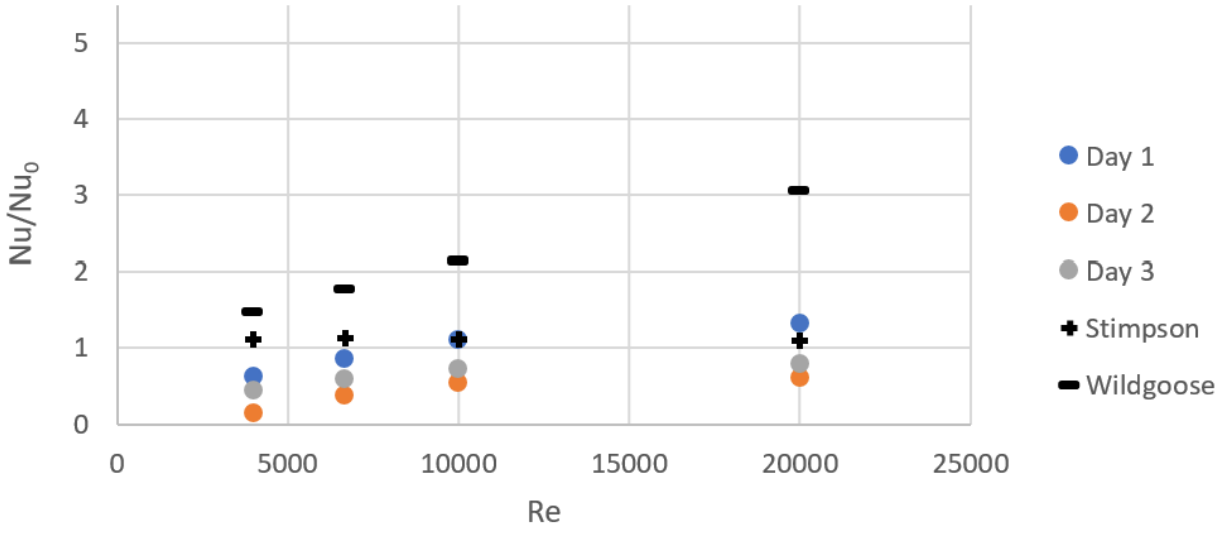

Figure **1-14**: Three test day results of channel 2 normalized Nusselt number over a range of Reynolds numbers.

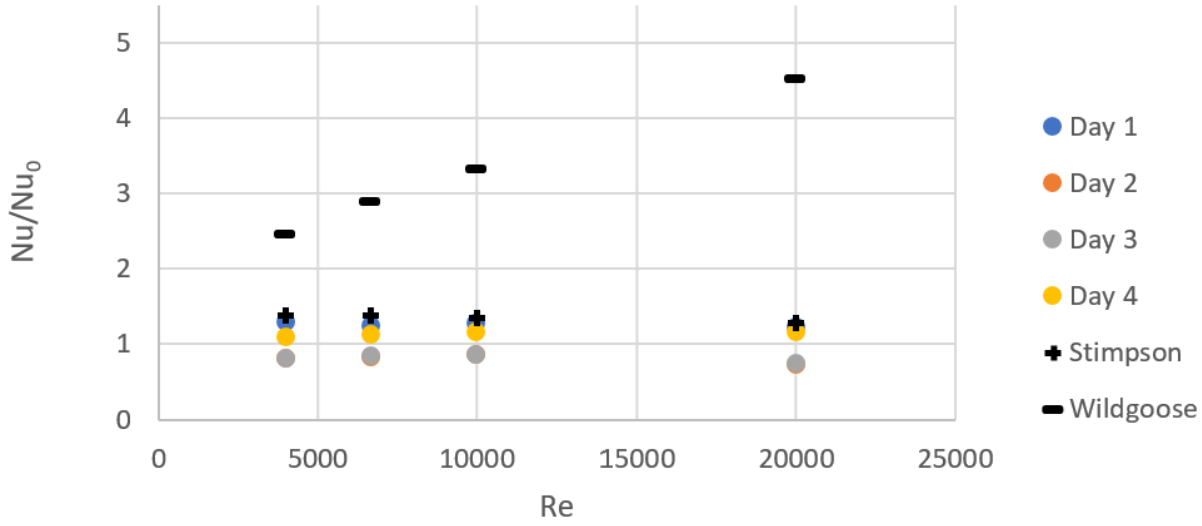

Figure **1-15**: Four test day results of channel 3 normalized Nusselt number over a range of Reynolds numbers.

1.6 Conclusion

Internal cooling is a necessary technology to include in the development of gas turbine blade hardware. Without internal cooling design features, turbine blades would be unable to withstand high gas temperatures. Recent trends show a continued increase in engine temperatures, which requires a parallel increase in internal cooling efficiency of turbine blades. The current study provides a developed methodology for heat transfer analysis of a variety of internal cooling design schemes. The methodology was developed with the aid of a 3D computational tool, where internal cooling schemes were evaluated via an analysis of 1x scale, linear cascade blade hardware. Seven total internal cooling schemes were incorporated into seven separate linear cascade blade hardware designs. The internal cooling schemes include several pin fin geometries, rib geometries, and channel design contours. Specifically, an empty channel hardware design was utilized in the evaluation of heat effects with CFD. It was determined that CFD internal air

temperature and internal heat transfer results aligned closely with that of the current study's developed methodology. Therefore, the methodology to calculate heat transfer in the present study has been validated according to computational methods. However, further and future testing of the cooling hardware designs must be completed in the high speed linear cascade to further validate the used methodology. An essential goal will be to develop a more accurate technique of obtaining the channel exit thermocouple measurements in the linear cascade to produce repeatable microchannel Nusselt number results.

References

[1] Kirsch, K. L., & Thole, K. A. (2017). Pressure loss and heat transfer performance for additively and conventionally manufactured pin fin arrays. *International Journal of Heat and Mass Transfer*, *108*, 2502–2513. https://doi.org/10.1016/j.ijheatmasstransfer.2017.01.095

[2] Ferster, K. K., Kirsch, K. L., & Thole, K. A. (2018). Effects of geometry, spacing, and number of pin fins in additively manufactured microchannel pin fin arrays. *Journal of Turbomachinery*, *140*(1), 1–10. https://doi.org/10.1115/1.4038179

[3] Wright, L. M., Fu, W. L., & Han, J. C. (2004). Thermal performance of angled, V-shaped, and W-shaped rib turbulators in rotating rectangular cooling channels (AR=4:1). *Journal of Turbomachinery*, *126*(4), 604–614. https://doi.org/10.1115/1.1791286

[4] Pham, K. Q., Nguyen, Q. H., Vu, T. D., & Dinh, C. T. (2020). Effects of Boot-Shaped Rib on Heat Transfer Characteristics of Internal Cooling Turbine Blades. *Journal of Heat Transfer*, *142*(10), 1–10. https://doi.org/10.1115/1.4047490

[5] Kirsch, K. L., & Thole, K. A. (2017). Heat transfer and pressure loss measurements in additively manufactured wavy microchannels. *Journal of Turbomachinery*, *139*(1). https://doi.org/10.1115/1.4034342

[6] Corbett, T., Thole, K. A., & Bollapragada, S. (2022). Amplitude and Wavelength Effects for Wavy Channels. *Journal of Turbomachinery*, 1–28. https://doi.org/10.1115/1.4055612

[7] Huelsmann, N. C., & Thole, K. A. (2021). Effects of jet impingement on convective heat transfer in effusion holes. *Journal of Turbomachinery*, *143*(6), 1–9. https://doi.org/10.1115/1.4050335

[8] Hossain, M. A., Ameri, A., Gregory, J. W., & Bons, J. P. (2021). Experimental investigation of innovative cooling schemes on an additively manufactured engine scale

turbine nozzle guide vane. *Journal of Turbomachinery*, *143*(5), 1–14. https://doi.org/10.1115/1.4049618

[9] Nirmalan, N. V., Bunker, R. S., & Hedlund, C. R. (2003). The measurement of full-surface internal heat transfer coefficients for turbine airfoils using a nondestructive thermal inertia technique. *Journal of Turbomachinery*, *125*(1), 83–89. https://doi.org/10.1115/1.1515798

[10] Egger, C., von Wolfersdorf, J., & Schnieder, M. (2013). Heat transfer measurements in an internal cooling system using a transient technique with infrared thermography. *Journal of Turbomachinery*, *135*(3), 1–8. https://doi.org/10.1115/1.4007625

[11] Zuccarello, J., Saltzman, D., Lynch, S. P., Haydt, S., Whitfield, C., "A Steady Transonic Linear Cascade for True Scale Cooling Measurements," Proceedings of ASME Turbo Expo 2020: Turbomachinery Technical Conference and Exposition, London, UK, GT2020-14269, 2020. https://doi.org/10.1115/GT2020-14269

[12] Rusted, A., & Lynch, S. (2021). Determining Total Pressure Fields from Velocimetry Measurements in a Transonic Turbine Flowfield. Proceedings of ASME Turbo Expo 2021: Turbomachinery Technical Conference and Exposition. 1-12. https://doi.org/10.1115/GT2021-59388

[13] King, et al., inventors. *S-Shaped Trip Strips in Internally Cooled Components*. 18 Dec. 2018. U.S. Patent 10,156,157 B2. https://patents.google.com/patent/US10156157B2/en

[14] Wildgoose, A. J., Thole, K. A., Sanders, P., & Wang, L. (2021). Impact of additive manufacturing on internal cooling channels with varying diameters and build directions. *Journal of Turbomachinery*, *143*(7), 1–11. https://doi.org/10.1115/1.4050336

[15] Stimpson, C. K., Snyder, J. C., Thole, K. A., & Mongillo, D. (2016). Roughness effects on flow and heat transfer for additively manufactured channels. *Journal of Turbomachinery*, *138*(5), 1–10. https://doi.org/10.1115/1.4032167